Supercond. Sci. Technol. 6 (1993) 246–249. Printed in the UK

Very thin $YBa_2Cu_3O_7$ step-edge Josephson junctions

H Kohlstedt, J Schubert, K Herrmann, M Siegel, C A Copetti, W Zander and A I Braginski
Institut für Schicht und Ionentechnik, Forschungszentrum Jülich (KFA), PO Box 1913, D-W5170 Jülich, Federal Republic of Germany

Received 4 January 1993

Abstract: Step-edge Josephson junctions were fabricated from 20 and 10 nm thick epitaxial $YBa_2Cu_3O_7$ films on $SrTiO_3$ substrates. The junction cross sections were in the 10^{-8} cm^2 range, similar to those in standard 200–300 nm thick junctions. The current–voltage characteristics, with and without microwave irradiation, were of resistively-shunted-junction (RSJ) type. The junction resistivities were in the range 10^{-8}–10^{-7} Ω cm^2 range, up to two orders of magnitude higher than in standard junctions, while the I_cR_ns were comparable. This behaviour was explained by a strong decrease in the number of parallel point-contact-type connections with the junction thickness. The junctions deteriorated quickly upon thermal cycling.

1. Introduction

In the last couple of years, the $YBa_2Cu_3O_7$ (YBCO) step-edge junctions (SEJ), first proposed by Simon *et al* [1], have been a widely investigated version of high-temperature superconducting (HTS) grain-boundary devices. Indeed, it has been shown that in epitaxial YBCO films grown on sufficiently steep steps in well-matched single-crystalline substrates, such as $SrTiO_3$ and $LaAlO_3$, two 90° grain boundaries are present [2, 3]. The current–voltage (I–V) characteristics and Josephson radiation spectra of these junctions indicate that they usually consist of two weak links in series [4, 5]. Hence, it is believed that each of the two 90° grain boundaries can exhibit a weak link behaviour. The junctions characterized thus far, used mainly in superconducting quantum interference devices (SQUIDs), have typically been fabricated from YBCO films 100–300 nm thick.

The purpose of our present work was to characterize SEJs fabricated from films which were an order of magnitude thinner, down to 10 nm. The motivation was to obtain junctions which could be used to extend the study of HTS superconducting field-effect transistor (SuFET) devices [6, 7] to Josephson FETs (JoFETs). As the carrier-density in a weak link region is much lower than in the film itself, the electric field screening should be reduced there and the field effect correspondingly enhanced. Indeed, the effectiveness of incorporating polycrystalline weak links into a JoFET structure fabricated from thin epitaxial YBCO film has been most recently demonstrated by Mannhart *et al* [8].

2. Fabrication and measurements

The steps in $SrTiO_3$ substrates were fabricated either by Ar^+-ion milling through photolithographically fabricated Nb masks [9] or the homoepitaxial step-edge junction (HESEJ) step fabrication technique [10]. The step heights were $h = 30$–90 nm. The very thin YBCO films were deposited by pulsed laser deposition. Down to the film thickness of $d = 20$ nm, no degradation of film properties was observed: the critical temperature (of zero resistance) was $T_{c0} = 88$ K and the critical current density $J_c > 4 \times 10^6$ A cm^{-2} ($T = 77$ K). At the thickness of 7 nm, $T_{c0} \approx 70$ K. The average film thickness was deduced from the number of laser pulses. The thickness per pulse was calibrated by Rutherford backscattering and profilometer measurements on much thicker films.

We initially patterned the junction microbridges in the very thin YBCO films by the standard photolithographic and Ar^+-milling process used to fabricate SEJs [9]. However, thin microbridges fabricated in this way remained resistive down to 4.2 K. Apparently, film heating in vacuum during ion-milling produced excessive damage in the weak link(s). Subsequently, we used an improved inhibit-patterning technique in which any exposure to heat and vacuum after the film deposition is avoided [11]. When using this method, 20 nm thick microbridges without steps remained undegraded down to a bridge width of 1 μm. In the present case, microbridges patterned across steps were 10 to 50 μm wide. This width range was chosen to maintain the standard junction cross section, of the order of 10^{-8} cm^2, and

0953-2048/93/040246 + 04 $07.50

maximize the chances that the, usually non-uniform [4], weak links remain superconducting. Our standard SEJ width range is 2–5 μm. For protection, 20 nm thick microbridges on HESEJ-type steps were coated *in situ* with a 200–300 nm thick amorphous α-$SrTiO_3$ layer, to alleviate the effect of the homoepitaxial $SrTiO_3$ roughness which was responsible for a high number of defects in the thin YBCO film. The 10 nm microbridges were fabricated only on ion-milled steps and had no protective coating. The gold contact pads were deposited *ex situ*. Several microbridges fabricated in this way were characterized as follows. Transport measurements of the I–V characteristics were performed using the conventional four-point method. Measurements of all 10 nm and some 20 nm thick samples were performed in a mumetal-shielded sample holder. In the absence of shielding flux trapping was the cause of the observed I–V curve assymetry and of a somewhat reduced I_c. The junction normal resistance, R_n, has been determined from the slope of the I–V characteristic obtained upon the complete suppression of the junction critical current, I_c, by microwave irradiation.

3. Results

We characterized microbridge SEJs fabricated from YBCO films 20 and 10 nm thick. Figure 1 shows an I–V characteristic measured at $T = 4.2$ K with and without 4.5 GHz irradiation in a 20 nm thick and 20 μm wide HESEJ microbridge with a step height of 90 nm ($d/h \approx 0.22$). Without irradiation, the characteristic is of a resistively-shunted-junction (RSJ) type and exhibits a hysteretic behaviour, also seen in standard SEJs having high J_c values and $I_c R_n$ products $\geqslant 2$ mV [4, 9]. However, the junction of figure 1 has a much lower average J_c (4.2 K) $= 8.8 \times 10^3$ A cm^{-2} (measured in the magnetic shield) and an $I_c R_n \approx 0.6$ mV at 4.2 K. The hysteresis was seen in this and other 20 nm thick junctions up to about 40 K while in standard devices on $SrTiO_3$, which operate up to 85 K, it is typically observed below about 20 K, i.e. at low normalized temperatures $t < 0.25$. The 20 nm thick junctions were superconducting only up to $T \leqslant 65$ K, approximately, so that the hysteretic behaviour persisted up to $t \geqslant 0.6$. Figure 2 shows a comparison of I–V curves of another 20 nm thick HESEJ junction ($w = 20$ μm, $d/h = 0.66$) measured at 4.2 and 53 K. The remarkably sharp I–V characteristic measured at 53 K is not hysteretic, in contrast to that recorded at 4.2 K.

Returning to figure 1, the I–V characteristic measured in the presence of irradiation shows two slopes corresponding to R_n values of, approximately, 13 and 23 Ω. The R_n change occurs at a voltage bias (indicated by an arrow) where the current through the second weak link in this SEJ exceeds its I_c.

The 10 nm thick, uncoated junctions had I_c values below 10 μA at 4.2 K and were not hysteretic. These junctions were not coated with α-$SrTiO_3$. Figure 3 shows an example of I–V curves recorded at 18 K, with

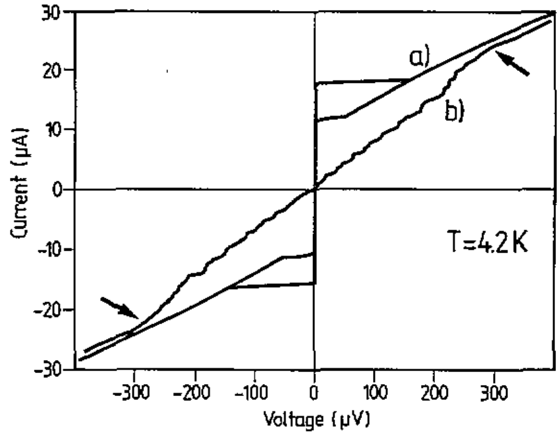

Figure 1. Current–voltage characteristics of a 20 nm thick and 20 μm wide SEJ ($d/h \approx 0.22$) measured (*a*) without and (*b*) with microwave radiation at a frequency of 4.5 GHz and a power of 13 dB m. The junction was coated with α-$SrTiO_3$.

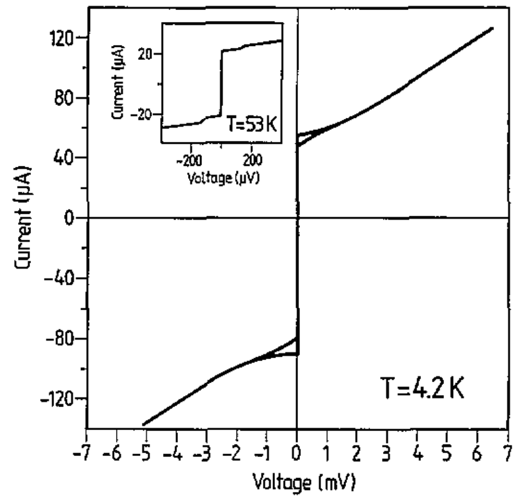

Figure 2. Current–voltage characteristic of a 20 nm thick and 20 μm wide SEJ ($d/h \approx 0.66$) at 4.2 K. The inset shows the current–voltage characteristic of the same junction at 53 K. The junction was coated with α-$SrTiO_3$.

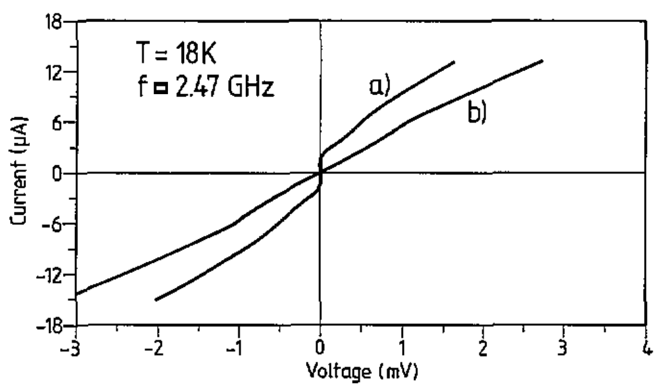

Figure 3. Current–voltage characteristics of an uncoated 10 nm thick and 10 μm wide SEJ (*a*) without and (*b*) with microwave radiation. The microwave frequency was 2.47 GHz.

and without 2.47 GHz irradiation. The measured junction was 16 μm wide and had a $d/h \approx 0.3$. It remained superconducting up to $T > 31$ K. The I–V curve measured with irradiation again shows the change in slope when the second weak link becomes resistive.

The normalized temperature dependence of the $I_c R_n$ product in the junction of figure 1 is shown in figure 4 (data recorded with shielding). The data points fit reasonably well Kupriyanov's SNS model with the barrier transparency parameter $\gamma_B = 30$ [12] and, in this respect, do not differ from those of a typical 200 nm thick junction for which the $I_c R_n$ data points are also shown. The superconductor/barrier boundary resistances should thus have been comparable. Indeed, the $I_c R_n$ products at 4.2 K were not much lower: 0.2 to >1.3 mV at 20 nm and up to 0.5 mV at 10 nm thickness. However, all thin junction resistances were in all cases one to two orders of magnitude higher and the I_c values lower than in 200 nm junctions. In 20 nm thick junctions, $R_n = 13$–$40\ \Omega$ and in junctions 10 nm thick $R_n = 100$–$200\ \Omega$. Thus far, the highest value of $I_c R_n >$ 1.3 mV at 4.2 K was measured in a 20 nm thick SEJ with $d/h = 0.66$, typical of standard SEJs.

Figure 5 shows Shapiro steps induced in the I–V characteristic of the junction of figure 2 exposed to $f = 5$ GHz radiation at various microwave power levels. The voltages of the very sharp current steps correspond to the Josephson relation $V = nfh/2e$, where h is Planck's constant, e the electron charge and $n = 1, 2, 3, \ldots$. Such sharpness of steps, not seen in standard SEJs, is reminiscent of those in low-temperature point-contacts. Over the limited range of microwave power used, the data of figure 3 could be well fitted to the RSJ model of a single junction. However, data of another such junction could only be fitted when assuming a parallel connection of at least two junctions. In the case, the I_c dependence on the magnetic field intensity $I_c(H)$ exhibited a SQUID-like behaviour.

All measured junctions degraded quickly with time. The uncoated 10 nm thick junctions, measured immediately after the last fabrication step, were no longer superconducting after 24 h or so, when subject to a

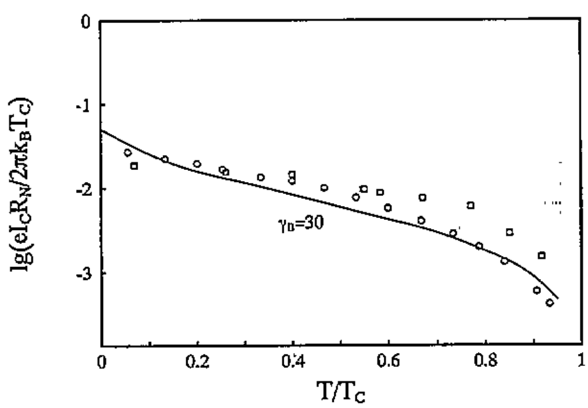

Figure 4. Normalized temperature dependences of the $I_c R_n$ product in a 20 nm (□) thick and a 200 nm (○) thick SEJ junction. The full curve represents the theoretical curve for $\gamma_B = 30$ [12].

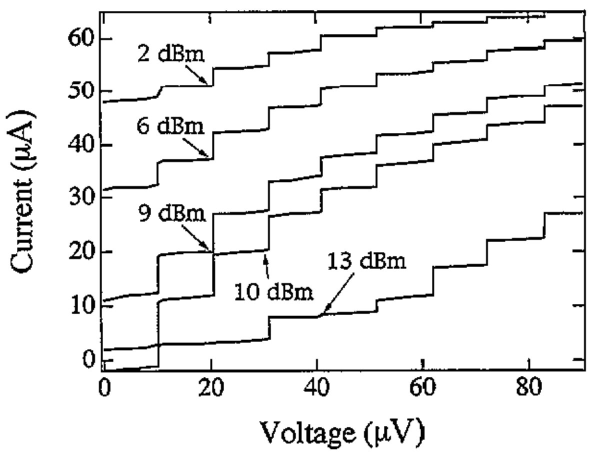

Figure 5. Shapiro steps induced in the current–voltage characteristic of the junction shown in figure 2 at different power levels and a frequency of 5 GHz.

second thermal cycle. The 20 nm junctions could be reliably measured over a period of several days when kept at low temperatures. Each thermal cycle, however, resulted in a measurable degradation of I_c. The α-$SrTiO_3$ coating proved insufficient to prevent a quick degradation of defect-rich HESEJ-type junctions.

4. Discussion

The preliminary results presented here show clearly that ultra-thin step-edge junctions, potentially suitable for JoFETs, can be fabricated with useful characteristics. The main problem, clearly not solved at present, is the quick degradation of uncoated and coated but defect-rich junctions. We hope that a solution to this problem can be found, at least for nearly defect-free films.

Independent of the practical usefulness of very thin SEJs, the results shown above raise an interesting question of importance for the understanding of this type of HTS junctions. While the thin junction cross sections are comparable to those of standard junctions, the average junction resistivities $\rho_n = R_n A$, where A is the cross-sectional area, differ considerably. The standard ρ_n values lie between 1×10^{-8} and $1 \times 10^{-9}\ \Omega\ \mathrm{cm}^2$ [9]. At $d = 20$ nm, we measured $\rho_n = 3$–$8 \times 10^{-8}\ \Omega\ \mathrm{cm}^2$, and at $d = 10$ nm $\rho_n \approx 2 \times 10^{-7}\ \Omega\ \mathrm{cm}^2$. Hence, the average ρ_n increases strongly with the decreasing film thickness. The scaling of $I_c R_n$ with $1/R_n$ usually observed in HTS grain-broundary junctions does not occur. A plausible explanation of this dependence assumes that SEJs are random parallel arrays of point contacts [4]. The number density of these point contacts appears to decrease with d, so that only a few or even one such point contact remains in very thin films (see the description of figure 3). The number of parallel connections across the 90° grain boundaries is thus increasing with the film thickness, i.e. the distance from the substrate.

The strongly hysteretic behaviour seen in figure 1 may possibly be caused by the enhanced stray capacitance in α-$SrTiO_3$-coated HESEJ junctions. An uncoated 20 nm thick junction did not exhibit a measurable hysteresis down to 4.2 K. Shunt capacitors with $SrTiO_3$/Ag deposited across SEJs were shown to increase the

Stewart–McCumber parameter to $\beta_c \approx 4$ at 4.2 K [13]. Apparently, even in the absence of the capacitor Ag-counterelectrode, the stray capacitance enhancement by a dielectric coating may increase β_c to well above one.

In the future, a more systematic work should address the issues raised here.

Acknowledgment

This work was supported, in part, by the BMFT Consortium 'First Application of HTS in Micro- and Cryoelectronics'.

References

[1] Simon R W *et al* 1990 *Science and Technology of Thin Film Superconductors 2* ed R D McConnell and R Noufi (New York: Plenum) p 549

[2] Jia C L, Kabius B, Urban K, Herrmann K, Cui G J, Schubert J, Zander W, Braginski A I and Heiden C 1991 *Physica* C **175** 545

[3] Jia C L, Kabius B, Urban K, Herrmann K, Schubert J, Zander W and Braginski A I 1992 *Physica* C **196** 212

[4] Siegel M, Herrmann K, Copetti C, Jia C L, Kabius B, Schubert J, Zander W and Braginski A I 1993 *IEEE Trans. Appl. Supercond.* **3** at press

[5] Reuter W, Siegel M, Herrmann K, Schubert J, Zander W, Braginski A I and Müller P 1993 *Appl. Phys. Lett.* at press

[6] Mannhart J G, Bednorz J G, Müller K A and Schlom D G 1991 *Z. Phys.* B **83** 307

[7] Xi X X, Li Q, Dought C, Kwon C, Bhattacharya S, Findikoglu A T and Venkatesan T 1991 *Appl. Phys. Lett.* **59** 3470

[8] Mannhart J, Ströbel J., Bednorz J G and Gerber Ch 1992 *Appl. Phys. Lett.* submitted

[9] Herrmann K, Zhang Y, Mück H M, Schubert J, Zander W and Braginski A I 1992 *Supercond. Sci. Technol.* **4** 583

[10] Schubert J and Zander W (KFA) unpublished

[11] Copetti C A, Gassig U, Zander W, Schubert J and Buchal Ch 1992 *Appl. Phys. Lett.* **61** 3041

[12] Kupriyanov M Yu and Likharev K K 1991 *IEEE Trans. Magn.* **MAG-27** 2460

[13] Daly K P, Burch J F, Hu R, Lee A E, Luine J and Petiette-Hall C 1993 *IEEE Trans. Appl. Supercond.* **3** at press